

Multiple Shape Coexistence in  $^{110,112}\text{Cd}$ 

P. E. Garrett,<sup>1,2</sup> T. R. Rodríguez,<sup>3</sup> A. Diaz Varela,<sup>1</sup> K. L. Green,<sup>1</sup> J. Bangay,<sup>1</sup> A. Finlay,<sup>1</sup> R. A. E. Austin,<sup>4</sup> G. C. Ball,<sup>5</sup> D. S. Bandyopadhyay,<sup>1</sup> V. Bildstein,<sup>1</sup> S. Colosimo,<sup>4</sup> D. S. Cross,<sup>6</sup> G. A. Demand,<sup>1</sup> P. Finlay,<sup>1</sup> A. B. Garnsworthy,<sup>5</sup> G. F. Grinyer,<sup>7</sup> G. Hackman,<sup>5</sup> B. Jigmeddorj,<sup>1</sup> J. Jolie,<sup>8</sup> W. D. Kulp,<sup>9</sup> K. G. Leach,<sup>1,\*</sup> A. C. Morton,<sup>5,†</sup> J. N. Orce,<sup>2</sup> C. J. Pearson,<sup>5</sup> A. A. Phillips,<sup>1</sup> A. J. Radich,<sup>1</sup> E. T. Rand,<sup>1,‡</sup> M. A. Schumaker,<sup>1</sup> C. E. Svensson,<sup>1</sup> C. Sumithrarachchi,<sup>1,†</sup> S. Triambak,<sup>2</sup> N. Warr,<sup>8</sup> J. Wong,<sup>1</sup> J. L. Wood,<sup>10</sup> and S. W. Yates<sup>11</sup>

<sup>1</sup>Department of Physics, University of Guelph, Guelph, Ontario N1G2W1, Canada

<sup>2</sup>Department of Physics and Astronomy, University of the Western Cape, P/B X17, Bellville ZA-7535, South Africa

<sup>3</sup>Departamento de Física Teórica and CIAFF, Universidad Autónoma de Madrid, E-28049 Madrid, Spain

<sup>4</sup>Department of Physics and Astronomy, St. Mary's University, Halifax, Nova Scotia B3H3C3, Canada

<sup>5</sup>TRIUMF, 4004 Wesbrook Mall, Vancouver, British Columbia V6T2A3, Canada

<sup>6</sup>Department of Chemistry, Simon Fraser University, Burnaby, British Columbia V5A1S6, Canada

<sup>7</sup>Department of Physics, University of Regina, Regina, Saskatchewan S4S0A2, Canada

<sup>8</sup>Institut für Kernphysik, Universität zu Köln, Zùlpicherstrasse 77, D-50937 Köln, Germany

<sup>9</sup>Defense Threat Reduction Agency, 8725 John J Kingman Road, Fort Belvoir, Virginia 22060-6217, USA

<sup>10</sup>Department of Physics, Georgia Institute of Technology, Atlanta, Georgia 30332, USA

<sup>11</sup>Departments of Chemistry and Physics and Astronomy, University of Kentucky, Lexington, Kentucky 40506-0055, USA



(Received 31 August 2018; revised manuscript received 29 June 2019; published 3 October 2019)

From detailed spectroscopy of  $^{110}\text{Cd}$  and  $^{112}\text{Cd}$  following the  $\beta^+$ /electron-capture decay of  $^{110,112}\text{In}$  and the  $\beta^-$  decay of  $^{112}\text{Ag}$ , very weak decay branches from nonyrast states are observed. The transition rates determined from the measured branching ratios and level lifetimes obtained with the Doppler-shift attenuation method following inelastic neutron scattering reveal collective enhancements that are suggestive of a series of rotational bands. In  $^{110}\text{Cd}$ , a  $\gamma$  band built on the shape-coexisting intruder configuration is suggested. For  $^{112}\text{Cd}$ , the  $2^+$  and  $3^+$  intruder  $\gamma$ -band members are suggested, the  $0_3^+$  band is extended to spin  $4^+$ , and the  $0_4^+$  band is identified. The results are interpreted using beyond-mean-field calculations employing the symmetry conserving configuration mixing method with the Gogny D1S energy density functional and with the suggestion that the Cd isotopes exhibit multiple shape coexistence.

DOI: 10.1103/PhysRevLett.123.142502

The shape of a nucleus is one of its most fundamental properties, and its exploration across the nuclear landscape provides insight into the mechanisms underlying how protons and neutrons are organized. Unlike atomic systems, which are exclusively spherical due to the  $1/r$  potential generated by the pointlike nucleus, nuclear shapes can be complicated because the potential is generated by the nucleons themselves. Minima in the total energy can be found for shapes that include spherical, axially symmetric prolate- or oblate-deformed ellipsoids, axially nonsymmetric (triaxial) ellipsoids, etc. Unlike other finite-bodied quantum-mechanical systems, a nucleus can exhibit different shapes for individual states, i.e., shape coexistence.

Shape coexistence, for which the most common form is the appearance of two distinct shapes, was long viewed as a rare and exotic phenomenon but has now been discovered spanning the nuclear chart (see, e.g., Ref. [1] for a recent review). Typically, the coexisting shapes are associated with a weakly deformed, and often spherical, ground state and a more deformed excited state upon which rotational states can be built. The reason that this form of shape

coexistence is the most prevalent is related to the fact that it is usually easier to identify a rotational band in a region of low level density of excited states (built on a spherical ground state) than vice versa. Since the driving mechanism behind the development of deformation is the strong proton-neutron quadrupole-quadrupole interaction at (or near) closed major shells, where the number of valence particles is zero (or small), the ground states have spherical (or weakly deformed) shapes, and the mechanism behind shape coexistence is often described as involving the promotion of pairs of particles across the large energy gap to orbitals above the shell closure. While the energy required to promote a pair of particles can be high, this may be offset by the gain in energy that arises from correlations, especially those associated with pairing, the neutron-proton interactions, and quadrupole deformation.

It is in the vicinity of closed major shells where the greatest abundance of shape-coexisting states have been sought and observed; an example of this occurs in the Sn region with its  $Z = 50$  closed proton shell [1,2]. The first nuclei in this region to be considered as candidates for

shape coexistence were the midshell Cd nuclei; the presence of a deformed band was experimentally established in  $^{110}\text{Cd}$  in Ref. [3]. The shape-coexisting states were labeled as *intruder* excitations, and they reach a minimum in excitation energy at the neutron midshell at  $N = 66$  ( $^{114}\text{Cd}$ ). Systematic studies of the even-even Cd isotopes focused largely on the vibrational aspects and the shape-coexisting intruder bands (see Refs. [1,2,4] for reviews).

Examples of multiple shape coexistence, where three or more distinct shapes occur, are rare, with the best examples to date in the Pb isotopes [1]; with  $^{186}\text{Pb}$  [5] as its epicenter, they are believed to possess prolate, oblate, and spherical states at low excitation energy. In the present Letter and the accompanying article [6], we suggest the possibility of multiple shape coexistence occurring in the Cd isotopes. This novel view of the structures of the Cd nuclei arises from detailed spectroscopy of highly nonyrast states combined with state-of-the-art beyond-mean-field (BMF) calculations. Unlike the Hg-Pb region, where the suggested triple shape coexistence occurs far from stability and presents extreme challenges to experimental study, detailed studies can be made of shape coexistence in the stable Cd isotopes.

To study the excited states in  $^{110,112}\text{Cd}$ , we employed both  $\beta$  decay and the  $(n, n'\gamma)$  reaction. The  $\beta^+$ /electron-capture decays of  $^{110,112}\text{In}$  and  $\beta^-$ -decay of  $^{112}\text{Ag}$  were studied at the TRIUMF-ISAC facility, where mass-separated beams of spallation products were deposited at the center of the  $8\pi$  spectrometer [7], which consisted of 20 high-purity Ge detectors with bismuth germanate Compton-suppression shields. Cycling of the beam deposition and tape movement was used to emphasize the decays of interest. For the mass 110 decay experiment, the beam delivered to the  $8\pi$  spectrometer consisted of  $1.2 \times 10^7 \text{ s}^{-1}$  of  $^{110}\text{In}^g$  ( $I^\pi = 7^+$ ,  $t_{1/2} = 4.9 \text{ h}$ ) and  $1.7 \times 10^6 \text{ s}^{-1}$  of  $^{110}\text{In}^m$  ( $I^\pi = 2^+$ ,  $t_{1/2} = 1.15 \text{ h}$ ). The results presented herein represent an extension of the work reported in Ref. [8], which focused on the decays of the lower-lying states. For the mass 112 decay measurement, an earlier experiment [9] was repeated and, while the ion beam rates were the same [ $7.5 \times 10^6 \text{ s}^{-1}$  of  $^{112}\text{In}^m$  ( $t_{1/2} = 20.6 \text{ min}$ ,  $I^\pi = 7^+$ ),  $2.3 \times 10^6 \text{ s}^{-1}$  of  $^{112}\text{In}^{gs}$  ( $t_{1/2} = 15 \text{ min}$ ,  $I^\pi = 1^+$ ), and  $4.8 \times 10^5 \text{ s}^{-1}$  of  $^{112}\text{Ag}$  ( $t_{1/2} = 3.1 \text{ h}$ ,  $I^\pi = 2^{(-)}$ ), the beam collection and decay times were altered in order to enhance the Ag decay in the data and minimize the background, resulting in a significant increase in sensitivity to  $^{112}\text{Ag}$  decay  $\gamma$  rays. Additional details can be found in Refs. [6,8].

Figure 1 displays selected results from the two decay experiments, with partial level schemes displayed in Figs. 2 and 3. The top panel of Fig. 1 shows a partial spectrum of  $\gamma$  rays in coincidence with the 1630 keV  $\gamma$  ray, corresponding to the  $2_4^+ \rightarrow 2_1^+$  transition in  $^{110}\text{Cd}$  where the presence of a 418 keV  $\gamma$  ray can clearly be seen. This  $\gamma$  ray is assigned as the 2706 keV ( $4_5^+$ )  $\rightarrow$  2287 keV ( $2_4^+$ ) transition. The

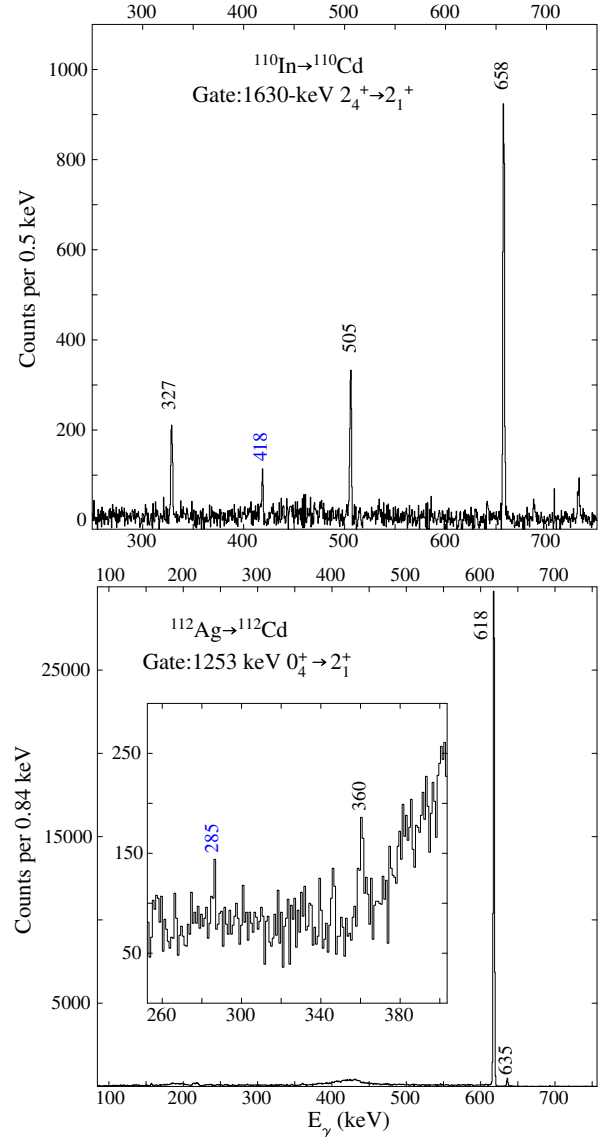


FIG. 1. Selected results from the present Letter for  $^{110}\text{Cd}$  (top) and  $^{112}\text{Cd}$  (bottom). (Top) Portions of the  $\gamma$ -ray spectrum in coincidence with the 1630 keV  $\gamma$  ray (the  $2_4^+ \rightarrow 2_1^+$  transition) in  $^{110}\text{Cd}$ . The 418 keV  $\gamma$  ray is assigned to the decay of the 2706 keV level (the  $4_5^+ \rightarrow 2_4^+$  transition). (bottom) Portion of the spectrum in coincidence with the 1253 keV  $\gamma$  ray (the  $0_4^+ \rightarrow 2_1^+$  transition) in  $^{112}\text{Cd}$ . The weak 285 keV  $\gamma$  ray assigned to the decay of the 2156 keV level ( $2_5^+ \rightarrow 0_4^+$  transition) is shown in the inset.

branching for this transition, 0.56(4)%, is determined using the gating from the below method [6,8]. The  $4^+$  assignment is confirmed from the observed decay of the 2706 keV state and its feeding from the 3240 keV  $6^+$  level. Lifetimes for levels in  $^{110}\text{Cd}$  are generally taken from Ref. [8] or Ref. [10]. Those for the 2287 keV  $2^+$ , 2706 keV  $4^+$ , and 2927 keV  $5^+$  states were determined via the Doppler-shift attenuation method following inelastic neutron scattering using the methods and procedures of Ref. [11], with the Doppler-shift data displayed in Ref. [6]. The reanalysis

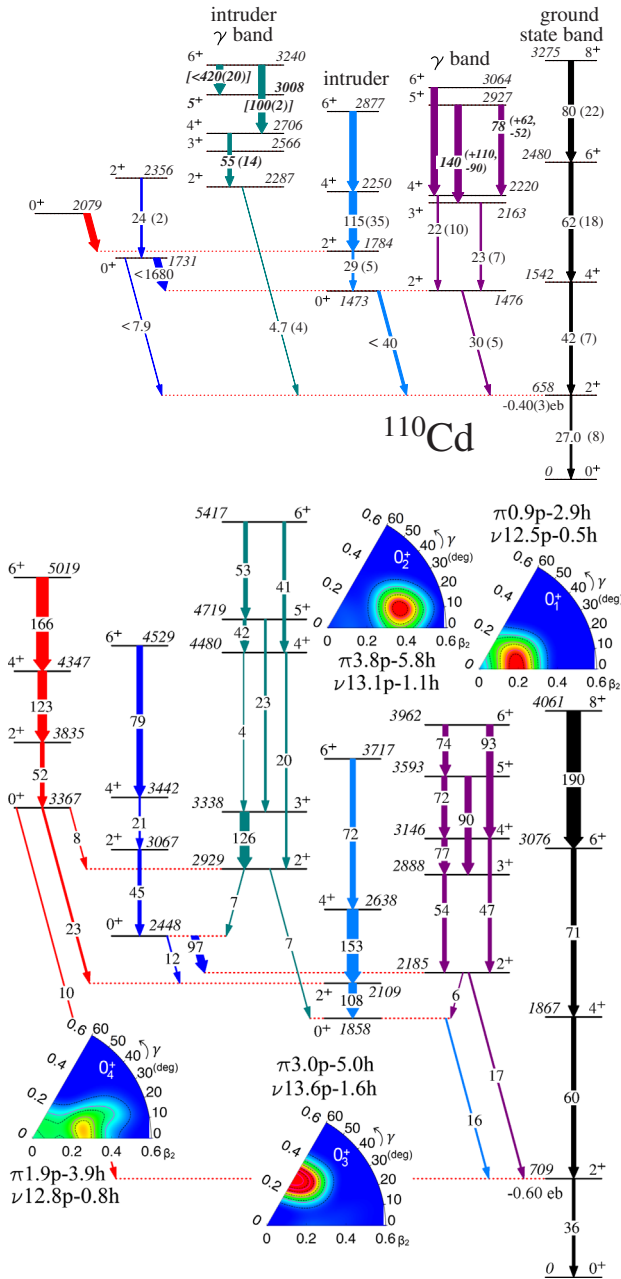


FIG. 2. The partial experimental level scheme deduced for  $^{110}\text{Cd}$  (top) and from the BMF calculation (bottom) showing the collective, low-lying, positive-parity bands with their in-band and bandhead decays. The transitions are labeled by  $B(E2)$  values in W.u. with uncertainties in parentheses; square brackets indicate relative values. Quantities in bold italic are newly determined. Upper limits result from lower limits for the level lifetimes, or unknown  $E2/M1$  mixing ratios, and the values given assume  $E2$  multipolarity. Also shown are the collective wave function distributions for the bandheads, plotted in the  $\beta - \gamma$  plane, with a color scheme of red for the maximum and blue for the minimum contribution. The average particle-hole occupation numbers extracted for protons ( $\pi$ ) and neutrons ( $\nu$ ) for the  $0^+$  states are indicated.

of the previously published data [12,13], as outlined in Ref. [8], yields lifetimes for the 2287, 2706, and 2927 keV levels of  $\tau = 395^{+30}_{-24}$ ,  $\tau = 221^{+68}_{-44}$ , and  $\tau = 245^{+500}_{-110}$  fs, respectively—the latter two determined for the first time. The extracted  $B(E2; 4_5^+ \rightarrow 2_4^+)$  of  $55 \pm 14$  W.u. indicates a large collective enhancement. Similarly, collective enhancements are observed for the decays of the 2927 keV  $5^+$  level to lower-lying  $3^+$ ,  $4^+$ , and  $6^+$  states. Also shown in Fig. 1 is a spectrum of  $\gamma$  rays in coincidence with the 1253 keV  $\gamma$  ray from the 1871 keV  $0_4^+$  state in  $^{112}\text{Cd}$ . The inset displays the 360 keV  $\gamma$ -ray peak that is assigned as the  $2_6^+ \rightarrow 0_4^+$  transition and a very small peak from a 285 keV  $\gamma$  ray that is assigned as the  $2_5^+ \rightarrow 0_4^+$  transition. The branching extracted for the latter is  $7.9(33) \times 10^{-4}$ , yielding  $B(E2; 2_5^+ \rightarrow 0_4^+) = 34(15)$  W.u. with the lifetime from Ref. [14]. Further analysis of the  $\gamma - \gamma$  coincidence data reveals a transition from the 2711 keV  $4^+$  state to the 2156 keV  $2^+$  level; its branching is deduced to be  $0.059 \pm 0.008$ , resulting in  $B(E2; 4_6^+ \rightarrow 2_5^+) = 77 \pm 30$  W.u. Further examples of coincidence spectra, and tables of the results, are found in Ref. [6].

The assignment of the levels into bands, as shown in Figs. 2 and 3, is generally based on the presence of an enhanced  $E2$  transition or a large relative  $B(E2)$  value. Exceptions to this practice are some of the levels associated with the intruder  $\gamma$  band. (Herein, we follow the convention of using the label of  $\gamma$  for the  $2^+$ ,  $3^+$ ,  $4^+$ , etc. ordering of states, independent of its exact nature as  $\gamma$  vibrational or nonaxial rotational.) In  $^{110}\text{Cd}$ , a sequence formed by the 2287 –  $2^+$ , 2566 –  $3^+$ , 2706 –  $4^+$ , 3008 –  $5^+$  (first observed in Ref. [15]), and 3240 keV –  $6^+$  states was observed, with an enhanced  $4^+ \rightarrow 2^+$  transition and a large  $6^+ \rightarrow 4^+$  branch. This sequence of levels is a candidate for the  $\gamma$  band based on the intruder  $0_2^+$  configuration, expected if the  $0_2^+$  level is indeed a deformed shape-coexisting state. In  $^{112}\text{Cd}$ , the  $2^+$  and  $3^+$  levels at 2231 and 2403 keV are considered as intruder  $\gamma$  band candidates; there is insufficient knowledge of higher spin levels to make suggested assignments. From the sensitivity achieved with the  $^{112}\text{Ag}$  decay, the  $0_3^+$  band in  $^{112}\text{Cd}$  has been extended to spin 4, and the  $0_4^+$  band has been located based on enhanced  $4^+ \rightarrow 2^+$  and  $2^+ \rightarrow 0^+$   $B(E2)$  values (see Ref. [6]).

The collective states are compared to the results of BMF calculations using the symmetry conserving configuration mixing method with the Gogny D1S energy density functional, as described in Ref. [16] and outlined in Ref. [6]. This is the first application of this method to the midshell nuclei in the  $Z = 50$  region that have previously been described as good spherical vibrators (see, e.g., Ref. [17]). The BMF effects are taken into account through the exact angular-momentum and particle-number restoration and include the possibility of axial and nonaxial shape mixing.

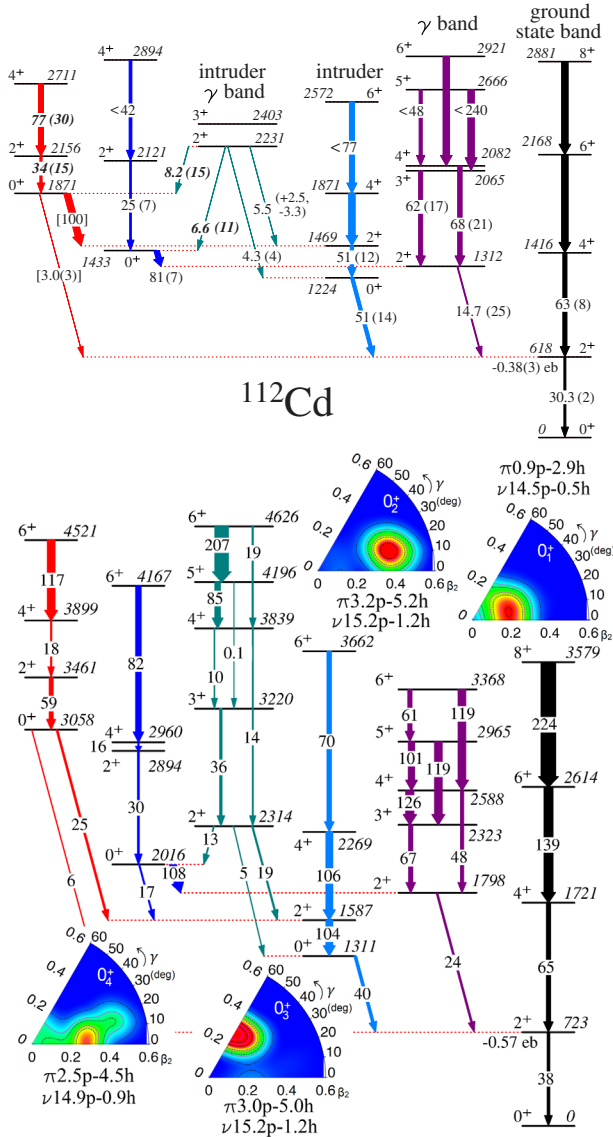


FIG. 3. The partial experimental level scheme deduced for  $^{112}\text{Cd}$  (top) and from the BMF calculation (bottom). See caption of Fig. 2 for details.

The occupation numbers are computed in a similar fashion as in Ref. [18] using the  $0s$ ,  $0p$ ,  $1s0d$ ,  $1p0f$ , and  $0g_{9/2}$  orbits as the reference to define the particle-hole structure for both protons and neutrons.

Rather than focus on the details, we concentrate on the overall gross features of the calculations. Considering that the calculations have no free parameters, there is remarkable similarity between the observed and predicted bands shown in Figs. 2 and 3. For both nuclei, four low-lying collective  $0^+$  states are predicted with distinct shapes: the prolate ground state band with  $\beta \approx 0.20$ , a triaxial-deformed  $0_2^+$  band with  $\beta \approx 0.4$  and  $\gamma \approx 20^\circ$ , an oblate  $0_3^+$  band with  $\beta \approx 0.30$ , and a prolate  $0_4^+$  band with  $\beta \approx 0.25$ . Two  $\gamma$  bands are also predicted, the lowest-lying

of which has  $\beta \approx 0.20$  (similar to the ground state) and triaxial, and the second band has a deformation nearly identical to that of the  $0_2^+$  state. The  $\gamma$  bands strongly mix in the calculations, resulting in enhanced  $E2$  transitions between the band members. There is also strong mixing of the spin 4 and 6 states of the  $0^+$  bands with states in other bands, especially those in close proximity, resulting in a fragmentation of the  $E2$  decay strength. The  $0_2^+$  states have enhanced  $E2$  transitions to the  $2_1^+$  states (predicted, 16 and 40 W.u.; observed,  $<40$  and  $51 \pm 14$  in  $^{110}\text{Cd}$  and  $^{112}\text{Cd}$ , respectively), the  $0_3^+$  bandheads have enhanced decays to the  $2^+$  bandheads of the  $\gamma$  bands (predicted 97 and 108 W.u., observed  $<1680$  and  $81 \pm 7$  W.u., respectively), and the  $0_4^+$  states have enhanced decays to the  $2^+$  member of the  $0_2^+$  band (23 and 25 W.u. predicted, and experimentally these  $E2$  transitions are favored by approximately 2 orders of magnitude versus other possible  $E2$  transitions).

The predicted energies of the states, as given in Figs. 2 and 3, are generally overestimated; this feature, however, is quite common in BMF calculations. The ratios of the  $4^+$  to  $2^+$  energies are 2.63 and 2.38 in  $^{110,112}\text{Cd}$ , respectively, whereas experimentally they appear slightly closer to the vibrational limit of 2.0 with values of 2.34 and 2.29. The in-band  $B(E2)$  values are also generally greater than observed, suggesting that the calculated deformation may be slightly too large, as also reflected in the quadrupole moments of the  $2_1^+$  states; the observed spectroscopic moments are  $-0.40(3)$  and  $-0.38(3)$   $eb$  for  $^{110,112}\text{Cd}$ , respectively, and the corresponding predicted values are  $-0.60$  and  $-0.57$   $eb$ .

A remarkable aspect of the present calculations is that they do not support spherical vibrational interpretations for the excited states of  $^{110,112}\text{Cd}$ ; the low-lying states are predicted to possess significant deformation and none of the states have vibrational wave functions. Detailed investigations of the Cd isotopes have revealed systematic discrepancies that are problematic to reconcile with their long-standing view as spherical vibrational systems [4,17,19]. Recently, the spherical vibrational interpretation was resurrected by considering terms in the Hamiltonian that mix phonon states, introducing a partial dynamical symmetry that preserves the typical spherical vibrator pattern for some states while allowing for departures for others [20]. In this model, the mixing with shape-coexisting intruder states remains weak, as reflected in the data [8]. The effect of the phonon mixing essentially interchanges the positions of the low-spin  $N+1$  and  $N$  phonon states. The  $0_3^+$  and  $0_4^+$  states, which would normally be members of the two- and three-phonon multiplets, respectively, interchange their characters, as do the  $2^+$  members of the three- and four-phonon multiplets. The present BMF calculations suggest an alternative explanation to the ‘‘Cd problem’’ [20], and the observation of enhanced  $B(E2)$  values supports their interpretation as rotational structures associated with the excited  $0^+$  states.



These results can be placed in the context of very recent Monte Carlo shell model (MCSM) calculations performed for the Sn isotope chain [21]. The Sn isotopes were long considered to be spherical and their structure described in the generalized seniority scheme [22,23]. However, the generalized seniority scheme does not reproduce the observed bump in the  $B(E2; 2_1^+ \rightarrow 0_1^+)$  values between  $N = 52$  and  $N = 64$ , nor did conventional shell model calculations [see, e.g., Fig. 2(a) of Ref. [21]]. By employing the MCSM, and keeping the full  $sdg$  shell, as well as the  $1h_{11/2}$ ,  $2f_{7/2}$ , and  $3p_{3/2}$  orbits, the trend in the  $B(E2)$  values was reproduced accurately. It was shown that the breaking of the  $Z = 50$  core is significant, especially for the  $1g_{9/2} \rightarrow 2d_{5/2}$  excitation, and this gives an enhancement to the  $E2$  matrix element. Further, when the ground state wave functions were analyzed using the so-called  $T$  plots, already at  $^{104}\text{Sn}$  significant deformation had emerged until  $N = 66$  was reached, at which point the seniority-zero states begin to dominate, and nearly spherical shapes are predicted due to a gradual widening of the  $Z = 50$  shell gap as the neutron number increases [21]. At  $N = 62$ , the average number of proton holes is  $\approx 0.5$  in the  $\pi 1g_{9/2}$  orbit [21]. In  $^{110,112}\text{Cd}$ , the BMF calculations predict an average proton ground state occupancy to be  $\pi(0.9p2.9h)$ , rather than the  $\pi(0p2h)$  that would result from a spherical Hartree-Fock calculation. The intruder band based on the  $0_2^+$  state, which is strongly populated in the Pd( $^3\text{He}, n$ ) two-proton transfer reaction [24], is calculated to have average occupancies of  $\pi(3.8p5.8h)$  in  $^{110}\text{Cd}$  and  $\pi(3.2p5.2h)$  in  $^{112}\text{Cd}$ , suggesting that the ground states of the Pd isotopes possess a structure more complicated than the  $\pi(4h)$  assumed for a spherical configuration. Extensive Coulomb excitation experiments [25] on the Pd isotopes yield ground state shape parameters of  $\beta = 0.24(2)$ , and  $\beta = 0.26(1)$  for  $^{108}\text{Pd}$  and  $^{110}\text{Pd}$ , consistent with a complicated  $\pi(ph)$  structure.

The suggested presence of multiple shape coexistence for the low-lying states in  $^{110,112}\text{Cd}$  provides an alternative interpretation of the structures observed and opens a new pathway for investigation of multiple shape coexistence in nuclei. For example, they can be explored by using highly sensitive Coulomb excitation and multinucleon transfer reactions. Within the broader context, if further experimental investigations confirm the multiple shape coexistence hypothesis proposed herein, it would provide further evidence that our view of the evolution of structure may need to be fundamentally altered. Rather than proceeding from spherical, closed-shell nuclei through a region of spherical vibrators before encountering deformation, deformation and shape coexistence may be confronted immediately, even at the closed shell. This is in-line with the recent MCSM results for the Sn isotopes [21] and also in the Ni isotopes (see, e.g., Refs. [26–28]), where indications of shape coexistence from experiment have been known for some time, and both the Monte Carlo and large-scale

phenomenological shell model calculations predict a similar scenario of excitation from the closed shells.

The assistance of Dr. F. Corminboeuf and Dr. L. Genilloud in the collection of the  $(n, n'\gamma)$  data is gratefully acknowledged, as are discussions with M. Zielińska and A. Gezerlis. This work was supported in part by the Natural Sciences and Engineering Research Council (Canada), TRIUMF through the National Research Council (Canada), and the U.S. National Science Foundation under Grant No. PHY-1606890. T. R. R. acknowledges computing time at GSI-Darmstadt and support from Spanish MINECO under FIS-2014-53434-P.

\*Present address: Department of Physics, Colorado School of Mines, 1523 Illinois Street, Golden, Colorado 80401, USA.

†Present address: National Superconducting Cyclotron Center, Michigan State University, East Lansing, Michigan 48824, USA.

‡Present address: Applied Physics Branch, Canadian Nuclear Laboratories, 286 Plant Road, Chalk River, Ontario K0J 1J0, Canada.

- [1] K. Heyde and J. L. Wood, *Rev. Mod. Phys.* **83**, 1467 (2011).
- [2] P. E. Garrett, *J. Phys. G* **43**, 084002 (2016).
- [3] R. Meyer and L. Peker, *Z. Phys. A* **283**, 379 (1977).
- [4] P. E. Garrett, J. L. Wood, and S. W. Yates, *Phys. Scr.* **93**, 063001 (2018).
- [5] A. N. Andreyev *et al.*, *Nature (London)* **405**, 430 (2000).
- [6] P. E. Garrett *et al.* (to be published).
- [7] P. E. Garrett *et al.*, *J. Phys. Conf. Ser.* **639**, 012006 (2015).
- [8] P. E. Garrett, J. Bangay, A. Diaz Varela, G. C. Ball, D. S. Cross, G. A. Demand, P. Finlay, A. B. Garnsworthy, K. L. Green, G. Hackman *et al.*, *Phys. Rev. C* **86**, 044304 (2012).
- [9] K. L. Green *et al.*, *Phys. Rev. C* **80**, 032502(R) (2009).
- [10] Data extracted from the National Nuclear Data Center, [www.nndc.bnl.gov](http://www.nndc.bnl.gov).
- [11] T. Belgya, G. Molnár, and S. W. Yates, *Nucl. Phys. A* **607**, 43 (1996).
- [12] F. Corminboeuf, T. B. Brown, L. Genilloud, C. D. Hannant, J. Jolie, J. Kern, N. Warr, and S. W. Yates, *Phys. Rev. Lett.* **84**, 4060 (2000).
- [13] F. Corminboeuf, T. B. Brown, L. Genilloud, C. D. Hannant, J. Jolie, J. Kern, N. Warr, and S. W. Yates, *Phys. Rev. C* **63**, 014305 (2000).
- [14] P. E. Garrett *et al.*, *Phys. Rev. C* **75**, 054310 (2007).
- [15] B. Jigmeddorj *et al.*, *Eur. Phys. J. A* **52**, 36 (2016).
- [16] T. R. Rodríguez and J. L. Egido, *Phys. Rev. C* **81**, 064323 (2010).
- [17] J. Kern, P. E. Garrett, J. Jolie, and H. Lehmann, *Nucl. Phys. A* **593**, 21 (1995).
- [18] T. R. Rodríguez, A. Poves, and F. Nowacki, *Phys. Rev. C* **93**, 054316 (2016).
- [19] P. E. Garrett, K. L. Green, and J. L. Wood, *Phys. Rev. C* **78**, 044307 (2008).
- [20] A. Leviatan *et al.*, *Eur. Phys. J. Web Conf.* **178**, 05003 (2018); *Phys. Rev. C* **98**, 031302(R) (2018).

- [21] T. Togashi, Y. Tsunoda, T. Otsuka, N. Shimizu, and M. Honma, *Phys. Rev. Lett.* **121**, 062501 (2018).
- [22] A. de-Shalit and I. Talmi, *Nuclear Shell Theory* (Academic Press, New York, 1963).
- [23] I. Talmi, *Nucl. Phys.* **A172**, 1 (1971).
- [24] H. W. Fielding, R. E. Anderson, C. D. Zafiratos, D. A. Lind, F. E. Cecil, H. H. Wieman, and W. P. Alford, *Nucl. Phys.* **A281**, 389 (1977).
- [25] L. Svensson, C. Fahlander, L. Hasselgren, A. Bäcklin, L. Westerberg, D. Cline, T. Czosnyka, C. Y. Wu, R. M. Diamond, and H. Kluge, *Nucl. Phys.* **A584**, 547 (1995).
- [26] S. Suchyta *et al.*, *Phys. Rev. C* **89**, 021301(R) (2014).
- [27] R. Taniuchi *et al.*, *Nature (London)* **569**, 53 (2019).
- [28] Y. Tsunoda *et al.*, *J. Phys. Soc. Jpn. Conf. Proc.* **23**, 013011 (2018).